Effects of motor pacing on frontal-hemodynamic responses during continuous upper-limb and whole-body movements

Ségolène Guérin, Marion Vincent, Yvonne Delevoye

Received: 11 May 2022 | Revised: 8 September 2022 | Accepted: 15 October 2022

DOI: 10.1111/psyp.14226

PSYCHOPHYSIOLOGY SPR WILEY

ORIGINAL ARTICLE

Effects of motor pacing on frontal-hemodynamic responses during continuous upper-limb and whole-body movements

Ségolène M. R. Guérin | **Marion A. Vincent** | **Yvonne N. Delevoye-Turrell**

Université de, UMR 9193 - SCALab - Sciences Cognitives et Sciences Affectives, France

Correspondence
Ségolène M. R. Guérin and Yvonne N. Delevoye-Turrell, SCALab - Sciences Cognitives et Sciences Affectives, University of Lille, UMR 9193, F-59000 Lille, France.
Email: segolene.guerin@univ-lille.fr (S. M. R. G) and yvonne.delevoye@univ-lille.fr (Y. N. D.-T.)

Funding information
Agence Nationale de la Recherche, Grant/Award Number: ANR-11-EQPX-0023; Centre National de la Recherche Scientifique, Grant/Award Number: CNRS 80PRIME-2020-KinAImotion; Université de Lille, Grant/Award Number: PhD ministerial grant 2018

Abstract

Advances in timing research advocate for the existence of two timing mechanisms (automatic vs. controlled) that are related to the level of cognitive control intervening for motor behavior regulation. In the present study, we used the functional near-infrared spectroscopy (*f*NIRS) cutting-edge technique to examine the hypothesis that prefrontal inhibitory control is needed to perform slow motor activities. Participants were asked to perform a sensorimotor-synchronization task at various paces (i.e., slow, close-to-spontaneous, fast). We contrasted upper-limb circle drawing to a more naturalistic behavior that required whole-body movements (i.e., steady-state walking). Results indicated that whole-body movements led to greater brain oxygenation over the motor regions when compared with upper-limb activities. The effect of motor pace was found in the walking task only, with more bilateral orbitofrontal and left dorsolateral activation at slow versus fast pace. Exploratory analyses revealed a positive correlation between the activation of the orbitofrontal and motor areas for the close-to-spontaneous pace in both tasks. Overall, results support the key role of prefrontal cognitive control in the production of slow whole-body movements. In addition, our findings confirm that upper-limb (laboratory-based) tasks might not be representative of those engaged during everyday-life motor behaviors. The *f*NIRS technique may be a valuable tool to decipher the neurocognitive mechanisms underlying naturalistic, adaptive motor behaviors.

KEYWORDS

cognitive control, ecological motor activity, *f*NIRS, inhibition, motor timing, sensorimotor synchronization, spontaneous pace

1 | INTRODUCTION

Locomotion is a fundamental behavior that consists in a robust motor pattern repeated over time. Experimental evidence has indicated that human beings perform routine locomotion behavior at ~2 Hz, which corresponds to two steps per second (MacDougall & Moore, 2005). This particular motor frequency has been referred to as the spontaneous motor tempo (i.e., the most natural and easiest pace to move; Fraisse, 1982; Moelants, 2002). Nonetheless,

individuals periodically need to accelerate or slow down the spontaneous pace of their actions in order to accommodate environmental constraints. For illustrative purposes, this is the case when trying not to miss a train or holding the hand of a toddler while walking down the street. The general aim of this article was to investigate the brain mechanisms underlying the temporal control of motor behaviors.

The way temporal control is applied over motor behaviors is still largely unknown. In the scientific literature, motor timing abilities have been commonly investigated using laboratory tasks that consist in artificial upper-limb movements (e.g., finger tapping; for a review, see Repp, 2005). Using upper-limb motor tasks, the production of fast motor behaviors (i.e., >2 Hz) was found to entail an automatic process in which the temporal regularities emerge from body dynamics (Lemoine, 2007; Lewis & Miall, 2003b). More precisely, Repp and Steinman (2010) stated that such *emergent timing* "arises from the dynamic control of nontemporal movement parameters such as stiffness" (p. 11). Thus, fast movements would be generated solely through motor dynamics without the need to internally control the timing of movements.

In contrast, the production of slow movements (i.e., <2 Hz) would originate from an explicit, cognitive representation of time. Such *predictive timing* is triggered by an "internal clock" that provides a sequence of periodic timing events independent of the effector(s) involved in motor production (Delignieres & Torre, 2011). Thus, the ability to perform slow movements requires cognitive control in order to apply voluntary control over motor behaviors (Bobin-Bègue & Provasi, 2008). More specifically, Bobin-Bègue et al. (2006) advocated that newborns and babies are unable to perform movements slower than their spontaneous pace because their motor inhibition function is not yet matured. We reached similar conclusions in a recent study in which we found that cognitive control is required for movements performed slower than the spontaneous motor pace. More precisely, using a sensorimotor-synchronization task in a dual-task paradigm, we reported that motor production at slow pace required more attentional resources than voluntary actions executed at close-to-spontaneous and fast paces in an adult population (Guérin, Boitout, & Delevoye-Turrell, 2021).

If emergent and predictive timing refer to two different timing mechanisms (emergent-automatic vs. predictive-controlled), they should involve two different patterns of neural activity. More specifically, emergent timing should be underpinned by cerebral structures that are characteristic of automatic, noncontrolled processes (e.g., motor areas; Saling & Phillips, 2007; Sumner & Husain, 2007). By contrast, predictive timing should involve brain areas representative of effortful, high-level cognitive processes (e.g., prefrontal cortex; Frith & Dolan, 1996; Koechlin et al., 2003). Following this train of thought, a couple of meta-analysis have indicated that motor tasks associated with emergent timing activate the motor system (e.g., supplementary motor area, basal ganglia) while those associated with predictive timing activate predominantly the frontal and parietal cortices (e.g., dorsolateral and ventrolateral prefrontal cortex, inferior parietal cortex; Lewis & Miall, 2003a, 2003b). It is noteworthy, however, that neuroimaging studies examining brain correlates of predictive timing used perceptual tasks (e.g., time estimation) while those investigating the neural substrate of emergent timing used upper-limb motor tasks (e.g., finger tapping). In the present study, we employed a unique motor task performed at various paces to test the hypothesis that prefrontal and motor regions will be differently engaged when moving fast and slow.

Brain imaging has been efficiently used to highlight the involvement of motor inhibition during go/no-go tasks (see e.g., Albares et al., 2014; Levin et al., 2014; Rubia et al., 2001). These studies found that the dorsolateral prefrontal and orbitofrontal cortices play a key role in inhibiting motor actions by modulating the strength of communication between prefrontal and motor regions (Rae et al., 2015). The go/no-go paradigm is easily implemented during brain recordings as it requires simple finger responses. Yet, it remains unclear whether the obtained results can be generalized to the temporal control of whole-body movements (e.g., walking) that mimic everyday-life behaviors and have a high ecological validity (see Sonkusare et al., 2019). Because they are so naturally and habitually performed, higher level of motor inhibition should be needed to apply a temporal control over naturalistic, whole-body movements. Nevertheless, popular neuroimaging methods (e.g., electroencephalography [EEG], functional magnetic resonance imaging [*f*MRI]) are highly sensitive to motion artifacts, which renders challenging the recording of cerebral activation during whole-body motor tasks (Herold et al., 2017, 2018).

*f*NIRS is a neuroimaging technique that enables the monitoring of brain activity in ecological whole-body movement paradigms (Herold et al., 2018; Perrey, 2014). This technique has several advantages over other imaging modalities that include low acquisition costs, continuous long-time monitoring, short installation time, portability, and higher robustness to motion artifacts (Leff et al., 2011). *f*NIRS makes use of the neurovascular coupling (i.e., the relationship between neuronal activation and subsequent changes in cerebral blood flow; Pasley & Freeman, 2008) to infer the magnitude

and spatial location of brain-cortical activity in response to experimental manipulations. In a previous study, we successfully used *f*NIRS to dissociate the involvement of different cognitive mechanisms as a function of task demands using a finger-tapping task (Guérin, Vincent, et al., 2021). More precisely, we found that actions produced at fast pace depended on motor activation while close-to-spontaneous movements led to higher posterior prefrontal activity. In addition, the hemodynamic responses recorded with *f*NIRS over the motor cortex were shown to be consistent with those reported using the same sensorimotor-synchronization tasks in *f*MRI (Rahimpour et al., 2020). Thus, *f*NIRS is a suitable tool to have a vista on the neurophysiological mechanisms involved in the pacing of whole-body movements.

The aim of the present study was to examine prefrontal and motor activity during the execution of continuous motor tasks at various tempi. Two tasks were used: a classic laboratory-based, upper-limb task (i.e., circle drawing) and a naturalistic, whole-body stepping-on-the-spot task (i.e., steady-state walking). Despite being characterized by contrasting ecological value, the drawing and walking tasks both belong to the category of continuous movements, defined as having "no recognizable beginning and end" (Schmidt et al., 1988, p. 46). These two motor tasks were executed in sensorimotor synchronization at fast (i.e., 300 ms), close-to-spontaneous (i.e., 600 ms), and slow paces (i.e., 1200 ms). Brain activity (i.e., oxygenated [HbO_2] and deoxygenated hemoglobin [HHb]) were recorded using the *f*NIRS technique over the bilateral primary motor and prefrontal cortices (i.e., orbitofrontal and dorsolateral regions) because of their involvement in inhibitory control.

It was hypothesized that steady-state walking will lead to a larger increase in HbO_2 over the primary motor cortex when compared to drawing due to the necessity to control whole-body musculature (H_1). Due to the involvement of high-level cognitive control and motor inhibition peculiar to predictive timing, performing movements at slow pace will lead to more prefrontal activation when compared with actions executed at close-to-spontaneous and fast paces (H_2). This effect will be magnified for movements that are deeply ingrained in human brain circuitry (i.e., steady-state walking), which will necessitate higher level of prefrontal control to be modulated (H_3). In addition, during both tasks, the slow tempi trials will lead to lower HbO_2 concentration in the motor areas than close-to-spontaneous and fast tempi trials (H_4), whose production depend on automatic, emergent timing (i.e., body dynamics). Exploratory analyses were also conducted to investigate (a) the possible relation between behavioral performance and HbO_2 concentration in the prefrontal cortex, and (b) the connection between HbO_2 in the prefrontal and motor regions.

2 | MATERIALS AND METHOD

2.1 | Participants

Healthy adults between 18 and 35 years ($M = 26$, $SD = 4.2$) were recruited for the present study among the staff and student corpus of the University of Lille. Inclusion criteria were normal to corrected-to-normal vision and the absence of motor dysfunctions, cardiovascular or endocrinological diseases, and neurological/psychiatric disorders. Participants were informed of the tasks that they would need to perform at least 48 h prior to inclusion. In addition, participants were asked not to consume caffeine on the day of the experimental session. After reading the information sheet, each participant was invited to provide written informed consent. At this point, participants were considered to be included in the experiment and demographic data were collected (i.e., sex, age). The ethics committee of the University of Lille (France) approved the study (reference 2017-8-S52).

The sample size required for the present study was calculated using G*Power (3.1.9.2). The *f*NIRS results of Guérin, Vincent, et al. (2021) were used as group parameters. The power analysis indicated that a total of 12 participants was required for the prefrontal activation ($f = .52$; $\alpha = .05$; $1 - \beta = .80$) and 9 participants for the motor activation ($f = .62$; $\alpha = .05$; $1 - \beta = .80$). Accordingly, a sample size of 12 participants was recruited. Three additional participants were included to guard against deletions due to experimental outliers.

The small telescopes approach was applied to determine the smallest effect size of interest (SESOI; Simonsohn, 2015) for each hypothesis. Accordingly, the SESOI was set to the effect size that an earlier study would have had 33% power to detect (Lakens et al., 2018). Once again, the *f*NIRS results of Guérin, Vincent, et al. (2021) were used. The sensitivity analysis indicated that an effect size of at least $f = .27$ (i.e., $\eta_p^2 = .07$) was required to yield meaningful results.

2.2 | Tasks description and materials

2.2.1 | Experimental procedure

Participants were administered two motor tasks: (a) a drawing task on a touchscreen and (b) a steady-state walking task. The experimental session took place in a quiet, windowless room that was dimly lit. Lighting is of

particular concern given that bright light can affect *f*NIRS signals (Shadgan et al., 2010).

For the drawing task, the touchscreen (1915 L Elo IntelliTouch 19″; Elo Touch Solutions Inc; Milpitas, California, CA) was placed on a table in front of the participant with the screen oriented at 45°. The participant was seated on a stool to minimize lower-limb muscular fatigue and avoid any extraneous movements during task performance. For the steady-walking task, the participant was asked to stand in the center of the room.

The *f*NIRS system (FOIRE-3000/16; Shimadzu, Kyoto, Japan) was placed behind the participant to limit distraction and facilitate the management of the cables. The cables were supported by an adjustable mechanical stand to carry the weight of the optical fibers (Coyle et al., 2007). This setup provided a means by which to ensure rigid *f*NIRS cable positioning, but also to minimize participant's strain and discomfort. A self-rated pain scale was also administered at the beginning and end of the experimental session. The scale was attached to a 9-point Likert pain scale, ranging from 1 (*no pain*) to 9 (*unbearable pain*). The participant was required to indicate the degree of pain that was experiencing in regard to the weight of the optodes on the head and neck.

2.2.2 | Task description

The two motor tasks were administered in a counterbalanced order across participants. In the drawing task, six targets (dots of 10-mm diameter) positioned around a 100-mm circle were display on the screen. The participant was required to trace the circle clockwise using the index finger with a closed fist. The participant was instructed to maintain accuracy in both temporal and spatial facets of the skill, but to favor temporal accuracy in case the task became too challenging for both to be maintained. In the walking task, the participant was asked to step on the spot.

The participant performed the drawing and steady-state walking tasks in synchrony with an auditory metronome set at three predefined tempi. The beeps of the metronome (duration = 80 ms, sound frequency = 294 Hz) were generated using Matlab 7.11.0 R2010 software (Mathworks Inc; Natick, Massachusetts). When the beep sounded, the participant was required to have: (a) their index finger of the dominant hand placed on the relevant target for the drawing task; (b) one foot on the ground for the walking task. For the latter, the participant was instructed to synchronize their right and left legs alternately.

The three tempi used in the study were 300 (i.e., fast tempo), 600 (i.e., close to spontaneous motor tempo), and 1200 ms (i.e., slow tempo). The fast- and slow-tempo trials enabled the participant to depart from their spontaneous motor tempo but remain within the possible sensorimotor-synchronization zone (between 180 ms and 1800 ms; Keele et al., 1985; Mates et al., 1994). Two Creative SBS 250 desk speakers (Creative Technology; Singapore) were used to play the metronome beeps.

2.2.3 | Experimental design

A block design procedure (i.e., alternating periods of activity and respite) was used in the present study. Each trial lasted 40 s and was preceded by a rest period varying between 25 and 35 s to allow the hemodynamic indices to return to baseline levels. The participant was presented with six blocks of three trials and was instructed to perform the drawing and steady-state walking tasks while synchronizing their movements to the metronome. Three blocks of trials were recorded for each task, with the slower, close-to-spontaneous, and faster conditions administered in a random order. Throughout the session, participants were encouraged not to speak and to avoid extraneous movements during each *f*NIRS trial. The total duration of the experimental test period was ~90 min.

2.3 | Data acquisition and preprocessing analyses

2.3.1 | Behavioral data

Drawing task

Data were collected using the touchscreen (sampling frequency = 100 Hz). Radii from the center of the circle to each target were computed. Points of interest were defined as the locus that intersects the participant's finger and each radius. Inter-response intervals (IRIs) were measured as the time interval between the onset of successive points of interest.

Walking task

Data were collected using six Oqus 5+ cameras (Qualisys MoCap, Göteborg, Sweden; sampling frequency = 50 Hz). A spherical passive marker was taped to the right participant's shoe to follow the movement of the foot. The recorded data were Cartesian coordinates (i.e., x, y, and z) and the points of interest were defined as the local maximum of z coordinates. IRIs were measured as the time interval between the onset of successive points of interest. Each IRI value was divided by two because only the right foot position was recorded.

Timing accuracy

Before conducting the main analyses, the time series was checked in order to detect and remove IRIs greater than twice the inter-stimuli interval (ISI) of a given block of trials (drawing = 12.63% of the IRIs, walking = 12.66% of the IRIs). These trials were referred to as temporal omissions and were not included in further analyses. An IRI_{error} was computed as the percentage of absolute difference between an IRI and its reference ISI for a given time interval i (see Equation 1).

$$IRI_{error(i)} = \frac{|IRI_i - ISI|}{ISI} \times 100 \quad (1)$$

The mean IRI_{error} measurement within a trial indicated the accuracy of time interval production (Repp, 2005).

2.3.2 | Headset position tracker

The position of the *f*NIRS headset was recorded using six Oqus 5+ cameras (Qualisys MoCap, Göteborg, Sweden) in the course of the entire experimental session. Specifically, one spherical passive marker was taped to the participant's right temple and two markers to the headset. The position for each marker was given in Cartesian coordinates (i.e., x, y, and z). The spatial accuracy of the system was 0.02 mm for each dimension of 3D space.

To verify the occurrence of an *f*NIRS headset shift, the surface of the planar triangle connecting the 3D markers was computed over a 30-s timing window (a) 30 s after the beginning of the experimental session and (b) 30 s before the end, following Equation 2:

$$\overrightarrow{M_0M_1}(t) \cdot \overrightarrow{M_0M_2}(t) = \begin{pmatrix} x_1(t)-x_0(t) \\ y_1(t)-y_0(t) \\ z_1(t)-z_0(t) \end{pmatrix} \cdot \begin{pmatrix} x_2(t)-x_0(t) \\ y_2(t)-y_0(t) \\ z_2(t)-z_0(t) \end{pmatrix} \quad (2)$$

where 0 = temple marker, 1 = first headset marker, 2 = second headset marker, and t = time point.

The percentage of variation between the two values was then calculated. An *f*NIRS headset shift was detected if this value exceeded 15% (for a similar procedure, see Guérin, Vincent, et al., 2021). If an *f*NIRS headset shift was detected, the behavioral and *f*NIRS data from the corresponding participant were removed prior to further analyses.

2.3.3 | Cardiorespiratory monitoring

Heart rate (HR) and respiration frequency were recorded to check the quality of the raw *f*NIRS signal (Pinti et al., 2019). Cardiorespiratory monitoring was conducted using an MP150 Biopac system (Biopac Systems, Goleta, CA), complemented with two dedicated add-on wearable devices. To facilitate acquisition, data were captured using a dual wireless respiration–electrocardiogram BioNomadix module. HR was captured by means of BN-EL45-LEAD3 lead set and two disposable patch electrodes placed on the participant's right and left clavicles. Respiration rate was recorded using a BN-RESP-XDCR respiration transducer. This respiratory belt was placed around the chest wall, below the sternum. The sampling frequency was set to 1000 Hz for both indices. Data acquisition was managed with the Acq*Knowledge* software.

2.4 | *f*NIRS data

2.4.1 | Data acquisition

Data were collected using a continuous-wave *f*NIRS system operating at three near-infrared wavelenghts (780, 805, and 830 nm) and monitored by the associated LabNIRS software. The sampling frequency was set at 2.27 Hz (i.e., temporal resolution of 440 ms). HbO_2 and HHb (mMol/L*cm) were computed in real time using Equations 3 and 4 (generated by LabNIRS from the modified Beer–Lambert law; Baker et al., 2014).

$$HbO_2 = (-1.4887) \times Abs[780\ nm] + 0.5970 \times Abs[805\ nm] + 1.4847 \times Abs[830\ nm] \quad (3)$$

$$HHb = 1.8545 \times Abs[780\ nm] + (-0.2394) \times Abs[805\ nm] + (-1.0947) \times Abs[830\ nm] \quad (4)$$

The fOLD toolbox (*f*NIRS Optodes' Location Decider; Morais et al., 2018) was used to guide the selection of optimal optode positioning with respect to the brain regions of interest, which were the bilateral orbitofrontal cortex (Brodmann's area 10, corresponding to the frontopolar area), dorsolateral prefrontal cortex (Brodmann's area 9), premotor cortex and supplementary motor area (SMA; Brodmann's area 6), and primary motor cortex (Brodmann's area 4). Thus, a 18-channel (11 light sources [multicomponent glass bundle fibers], 11 detectors [multi-alkali photomultipliers detectors]) configuration was designed in order to ensure an anatomical specificity of at least 30% for each region of interest (see Table 1 and Figure 1).

The optodes were attached to an *f*NIRS headset with a 3-cm source-detector distance, giving a depth of analysis between 0.5 and 2.0 cm. The headset was placed on each participant's head in accordance with the International 10–20 system guidelines for standard electrode positions

TABLE 1 Anatomical specificity for each channel

Channel	Source–detector	Specificity
1	Fpz–Fp1	Frontopolar area (54.5%), orbitofrontal area (44.9%)
2	Fpz–Fp2	Frontopolar area (54.5%), orbitofrontal area (44.8%)
3	AF3–F1	DLPFC (80.4%), frontopolar area (16.9%)
4	Fz–Afz	DLPFC (61.8%), frontopolar area (20.3%), FEF (12.1%)
5	AF4–F2	DLPFC (77.9%), frontopolar area (18.4%)
6	F3–F1	DLPFC (91.4%)
7	Fz–F1	DLPFC (63.2%), FEF (34.7%)
8	Fz–F2	DLPFC (68.9%), FEF (28.9%)
9	F4–F2	DLPFC (90.8%), FEF (5.6%)
10	F3–FC3	DLPFC (49.1%), Broca's area (41.2%), premotor cortex and SMA (6.8%)
11	F4–FC4	DLPFC (47.1%), Broca's area (42.1%), premotor cortex and SMA (7.6%)
12	FC1–FC3	Premotor cortex and SMA (37.5%), DLPFC (35.1%), FEF (23.5%)
13	FC1–FCz	Premotor cortex and SMA (73.2%), FEF (25.9%)
14	FC2–FCz	Premotor cortex and SMA (63.0%), FEF (35.3%)
15	FC2–FC4	Premotor cortex and SMA (38.2%), DLPFC (35.8%), FEF (21.5%)
16	C3–C1	Primary motor cortex (35.0%), premotor cortex and SMA (34.6%), primary somatosensory cortex (24.6%)
17	C4–C2	Primary motor cortex (36.8%), premotor cortex and SMA (29.5%), primary somatosensory cortex (25.6%)
18	Cz–CPz	Primary motor cortex (47.1%), somatosensory association cortex (29.1%), premotor cortex and SMA (10.5%)

Note: Information obtained from the fOLD toolbox (Morais et al., 2018). Only brain areas with >5% of specificity are reported.

Abbreviations: DLPFC, dorsolateral prefrontal cortex; FEF, frontal eye fields; SMA, supplementary motor area.

(Jasper, 1958). As a result, the Cz optode was located at the midway point between the nasion and inion. A stylus with a LED light was used to remove hair from each optode hole before the corresponding optode was wired to the *f*NIRS headset. This is of particular importance to avoid

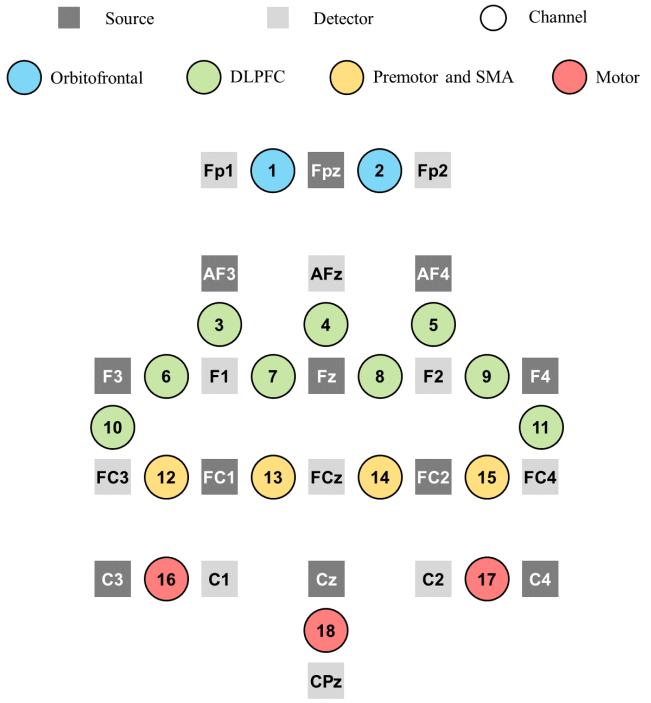

FIGURE 1 Diagrammatic representation of the sources, detectors, and channel layout. DLPFC, dorsolateral prefrontal cortex; SMA, supplementary motor area

light obstruction due to the presence of hair between the optode and participant's scalp.

System calibration was performed through an automatic adjustment using LabNIRS to adapt the internal parameters of the *f*NIRS device (e.g., gain, amount of light to emit) to the head morphology and the hair-type characteristics of each participant. Calibration was performed at the beginning of each experimental session. In case the amount of light detected was not sufficient, the hair was pushed back from beneath each problematic source–detector couple until the values were satisfactory.

2.4.2 | Data processing

To control for the quality of the acquired *f*NIRS data, the power-spectrum density was computed using the raw *f*NIRS intensities for each participant, trial, and channel. The frequency corresponding to maximal peak in the 50–160 beat-per-minute (bpm) range was detected visually. The identified frequencies were compared to the HR measurements provided by the Biopac system. A participant was removed from further analyses if HR frequency was not visible in the *f*NIRS signals. Nine participants were rejected on this basis. Note that any excluded participants were replaced to have a final sample size of $N = 15$.

The presence of the heart pulse is a necessary, but not sufficient condition to ensure the quality of *f*NIRS data. Thus, the QT-NIRS toolbox (Quality Testing of Near-Infrared Scans; Hernandez & Pollonini, 2020) was used to identify channels with poor optical coupling. More specifically, the scalp-coupling index was computed by use of the following parameters: cardiac filter = 0.5–2.27 Hz; time window = 5 s; λ = 805 and 830 nm.

The scalp-coupling index quantified the cross-correlation between the cardiac waveform of two wavelengths (i.e., 805 and 830 nm) for each channel over the entire trial (Pollonini et al., 2016). For a given participant and channel, trials with a scalp-coupling index <0.8 were removed prior to further analyses (trial = 5-s baseline + 40-s task). Overall, 1.72% of the trials was removed in accord with this criterion. For each participant and task, the entire channel was removed if <70% of the trials were ineligible; 1.88% of the channels pertaining to the brain region of interest was removed on this basis.

Correction for motion artifacts was performed using wavelet filtering (interquartile range = 1.5) in Homer 3 (partial pathlength factor = 1; v1.31.2; Massachusetts General Hospital, Boston, MA, USA). The motion-corrected data were visually inspected to ensure that the selected interquartile range value was well suited to the *f*NIRS data. A fourth-order Butterworth filter with a band pass of [0.001–0.2] Hz was applied to correct for physiological noise. The lowpass was set at 0.2 Hz to preserve the stimulation protocol frequency (1 / [task + mean rest] = 0.01 Hz) and the 2nd and 3rd harmonics without attenuation. HbO_2 and HHb data coming from trials characterized by <70% level of behavioral accuracy were removed from further calculations. The hemodynamic response function was then computed as the mean HbO_2 and HHb for each experimental condition using Matlab personal code.

For each hemodynamic response function, a baseline *B* and plateau *P* were defined for HbO_2 and HHb. More specifically, the mean values of the *f*NIRS signal were computed starting 5 s before the task onset and 5 s before its end for *B* and *P*, respectively. Both indices were computed upon a 5-s time window. Then, the HbO_2 and HHb variations $\Delta = B - P$ of an hemodynamic response function were computed (for similar calculations, see Derosière et al., 2014; Mandrick et al., 2013). Finally, the mean variations $\overline{\Delta}_{HbO_2}$ and $\overline{\Delta}_{HHb}$ were given for each regions of interest (i.e., bilateral orbitofrontal, dorsolateral prefrontal, primary motor cortices; see Table 1 and Figure 1 for more detailed information on the spatial registration and regions of interest).

2.5 | Statistical analyses

Because HbO_2 benefits from a better signal-to-noise ratio (see Gervain et al., 2011), only $\overline{\Delta}_{HbO_2}$ was used to support or refute hypotheses. Nonetheless, $\overline{\Delta}_{HHb}$ was also analyzed and the findings are reported in Supplementary File S1. The *f*NIRS-dependent variable $\overline{\Delta}_{HbO_2}$ was analyzed independently for each region of interest since the hemodynamic response function was found to differ among brain regions (see Kamran et al., 2015). IRI_{error} were analyzed only for the participants and trials with eligible *f*NIRS data.

To examine $H_1 - H_4$, a two-way repeated-measure analysis of variance (RM ANOVA; Motor Tempo [300, 600, 1200 ms] × Task [drawing, walking]) was applied to $\overline{\Delta}_{HbO_2}$. A similar RM ANOVA was employed to analyze the timing accuracy (i.e., IRI_{error}). Normality was checked using visual inspection of the quantile–quantile plots and the Shapiro–Wilk test. Where Mauchly's tests indicated violations of the sphericity assumption, Greenhouse–Geisser corrections were applied. Paired *t* tests with Bonferroni adjustements were used as post hoc tests where necessary. As exploratory analyses, the correlations between (a) IRI_{error} and $\overline{\Delta}_{HbO_{2,prefrontal}}$ concentration, and (b) $\overline{\Delta}_{HbO_{2,prefrontal}}$ and $\overline{\Delta}_{HbO_{2,motor}}$ were computed using Pearson's product–moment correlation. Pearson's correlation coefficients (*r*) were interpreted as follows: $r < .2$ was considered as an absence of correlation, $r < .4$ was considered low, $r < .6$ was considered moderate, $r < .8$ was considered moderately high, and $r \geq .8$ was considered high (Zhu, 2012). RStudio (v.1.2.5019) was used for the statistical analyses, with alpha set at $p < .05$.

3 | RESULTS

3.1 | *f*NIRS-headset shift

An *f*NIRS-headset shift was detected for one participant (see Figure 2). Data from this participant were removed prior to further analyses. For the remaining 24 participants,[1] the average variation of the *f*NIRS-headset positioning was 2.00% ($SD = 1.74$).

3.2 | Behavioral data

The RM ANOVA showed a significant main effect of motor tempo, $F(2, 22) = 6.93$, $p = .005$, $\eta_p^2 = .39$, with more IRI_{error} in the 300 ms ISI ($M = 17.14$, $SD = 7.88$) than in the 600 ($p = .013$, $M = 13.45$, $SD = 5.93$) and 1200 ms ISI conditions ($p = .005$, $M = 11.92$, $SD = 3.25$). The main effect of task was also significant, $F(1, 11) = 12.09$, $p = .005$, $\eta_p^2 = .52$, with greater IRI_{error} during the drawing ($M = 16.45$,

[1]In total, 25 participants were included in the study, but nine participants were excluded due to poor *f*NIRS optical coupling.

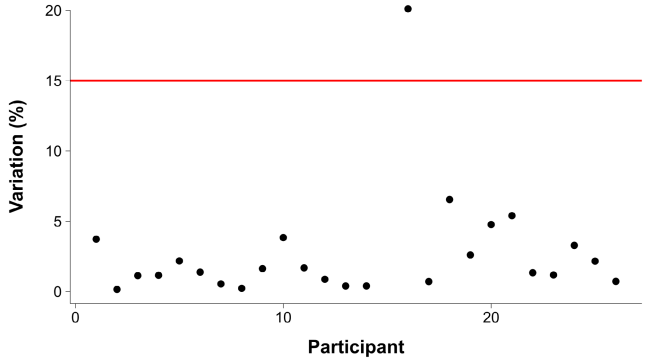

FIGURE 2 *f*NIRS-headset shift. Variation of the *f*NIRS-head positioning for each experimental condition and participant. The red line indicates the *f*NIRS headset shift threshold at which a given participant's data were removed prior to further analyses. Data from all participants included in the study are displayed (i.e., before exclusion due to poor optical coupling)

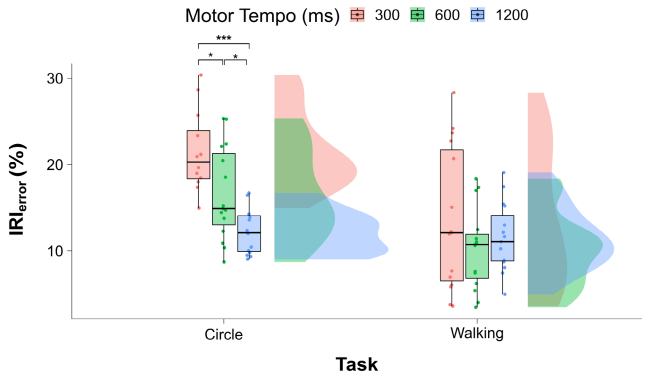

FIGURE 3 Timing accuracy for each experimental condition. Box plots and density distributions are displayed for each designated motor tempo and task. Each dot represents an individual participant. * $p < .050$, *** $p < .001$

SD = 5.64) than during the walking task ($p < .001$, $M = 11.84$, $SD = 5.98$).

The Motor Tempo × Task interaction was significant, $F(1.35, 14.85) = 8.02$, $p = .008$, $\eta_p^2 = .42$. This indicated that IRI_{error} was greater in the 300 vs. 600 ms ($p = .033$), 300 vs. 1200 ms ($p < .001$), and 600 vs. 1200 ms ISI conditions ($p = .014$) during the drawing task but not during the walking task. Overall, the results indicated that participants made more timing errors in the fast externally-paced tempo condition in the drawing task only (see Figure 3).

3.3 | *f*NIRS data

3.3.1 | Orbitofrontal cortex

The RM ANOVA did not show a significant main effect of task, $F(1, 11) = 2.28$, $p = .159$, $\eta_p^2 = .17$, or motor tempo, $F(1.26, 13.91) = 2.84$, $p = .108$, $\eta_p^2 = .20$. The Task × Motor Tempo interaction was significant, $F(2, 22) = 5.78$, $p = .010$, $\eta_p^2 = .34$, indicating that orbitofrontal cortex oxygenation was greater in the 1200 ($M = 2.09 \times 10^{-5}$; $SD = 1.50 \times 10^{-4}$) vs. 300 ms ISI conditions ($M = -1.19 \times 10^{-4}$; $SD = 1.61 \times 10^{-4}$; $p = .012$, Cohen's $d = 0.98$) only during the walking task (see Figure 4). Note that the effect size was larger than the required SESOI, indicating that the effect was sufficiently strong to yield meaningful results.

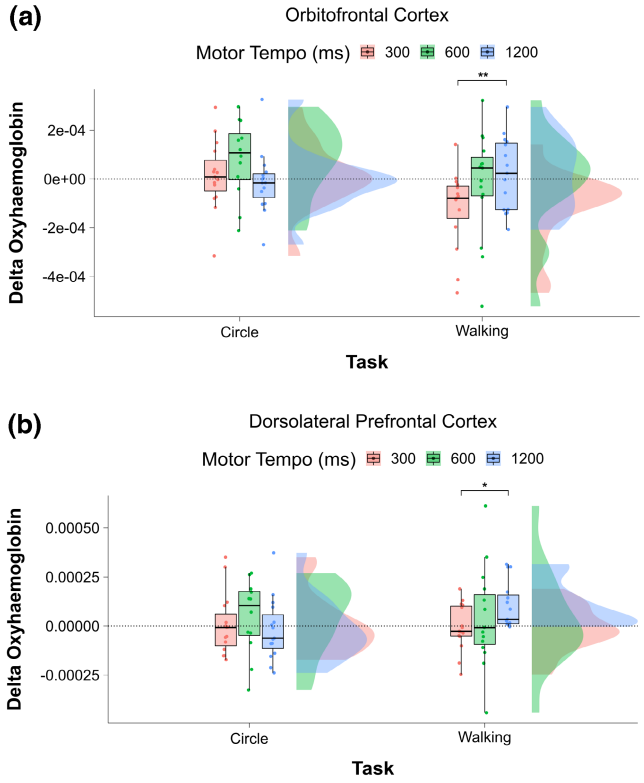

FIGURE 4 *f*NIRS results for the prefrontal cortex. Box plots and density distributions are displayed for each designated motor tempo and task. Each dot represents an individual participant. Panel A: Data for the orbitofrontal cortex. Panel B: Data for the dorsolateral prefrontal cortex. * $p < .050$, ** $p < .010$

3.3.2 | Dorsolateral prefrontal cortex

The RM ANOVA did not show a significant main effect of task, $F(1, 11) = 1.16$, $p = .305$, $\eta_p^2 = .09$, or motor tempo, $F(1.28, 14.04) = 0.85$, $p = .400$, $\eta_p^2 = .07$. The Task × Motor Tempo interaction was significant, $F(2, 22) = 4.14$, $p = .030$, $\eta_p^2 = .27$, indicating that the oxygenation of the dorsolateral prefrontal cortex was greater in the 1200 ($M = 1.03 \times 10^{-4}$; $SD = 1.18 \times 10^{-4}$) vs. 300 ms ISI conditions ($M = -7.1 \times 10^{-6}$; $SD = 1.19 \times 10^{-4}$; $p = .002$, Cohen's $d = 1.22$) only during the walking task (see Figure 4). Note that the effect size was larger than the required SESOI,

indicating that the effect was sufficiently strong to yield meaningful results.

3.3.3 | Premotor cortex and SMA

The RM ANOVA showed a significant main effect of task, $F(1, 11) = 7.55$, $p = .019$, $\eta_p^2 = .41$, with higher premotor cortex and supplementary motor area oxygenation in the walking ($M = 1.58 \times 10^{-4}$, $SD = 1.85 \times 10^{-4}$) than in the circle drawing task ($M = 4.43 \times 10^{-5}$, $SD = 1.87 \times 10^{-4}$, Cohen's $d = 0.48$; see Figure 5). The main effect of motor tempo was nonsignificant, $F(1.26, 13.9) = 0.66$, $p = .464$, $\eta_p^2 = .06$. The Task × Motor Tempo interaction was also nonsignificant, $F(2, 22) = 1.96$, $p = .164$, $\eta_p^2 = .15$.

3.3.4 | Primary motor cortex

The RM ANOVA showed a significant main effect of task, $F(1, 11) = 10.52$, $p = .008$, $\eta_p^2 = .49$, with greater primary motor cortex oxygenation during the walking ($M = 1.93 \times 10^{-4}$, $SD = 2.27 \times 10^{-4}$) than during the drawing task ($M = 5.01 \times 10^{-5}$, $SD = 2.38 \times 10^{-4}$, Cohen's $d = 0.51$; see Figure 5). The main effect of motor tempo was nonsignificant, $F(2, 22) = 0.70$, $p = .506$, $\eta_p^2 = .06$. The Task × Motor Tempo interaction was also nonsignificant, $F(2, 22) = 1.48$, $p = .250$, $\eta_p^2 = .12$. Note that the effect size was larger than the required SESOI, indicating that the effect was sufficiently strong to yield meaningful results.

3.4 | Exploratory analyses

3.4.1 | Correlations

To investigate the possible relation between behavioral performance and HbO_2 concentration, the linear correlation between the IRI_{error} and prefrontal activation in the slow walking trials was computed. Pearson's correlation coefficient was used ($\alpha = .05$) and the normality of the distributions was checked through visual inspection of the quantile–quantile plots. The correlation was nonsignificant for the bilateral orbitofrontal ($r = .27$, $t(13) = 1.02$, $p = .163$, $r^2 = .07$) and left dorsolateral prefrontal cortex ($r = .21$, $t(13) = .77$, $p = .227$, $r^2 = .04$).

Additional Pearson's correlation coefficients were computed to further examine the connection between the prefrontal and motor regions as a function of motor tempo during the walking task (Bonferroni corrected $\alpha = .05 / 3 = .017$). The correlation between the primary motor cortices and bilateral orbitofrontal oxygenation was significant in the close-to-spontaneous pace condition ($r = .68$, $t(13) = 3.36$, $p = .005$, $r^2 = .46$), but not in the slow ($r = .28$, $t(13) = 1.03$, $p = .320$, $r^2 = .08$) and fast pace conditions ($r = -.16$, $t(13) = -0.57$, $p = .575$, $r^2 = .02$; see Figure 6). In addition, the correlation between the oxygenation levels of the bilateral primary motor cortices and left dorsolateral prefrontal was significant in the slow ($r = .72$, $t(13) = 3.79$, $p = .002$, $r^2 = .52$) and close-to-spontaneous pace conditions ($r = .72$, $t(13) = 3.70$, $p = .003$, $r^2 = .51$), but not in the fast pace condition ($r = .55$, $t(13) = 2.38$, $p = .033$, $r^2 = .30$; see Figure 6).

The correlation between the premotor cortex and SMA, and bilateral orbitofrontal oxygenation was significant

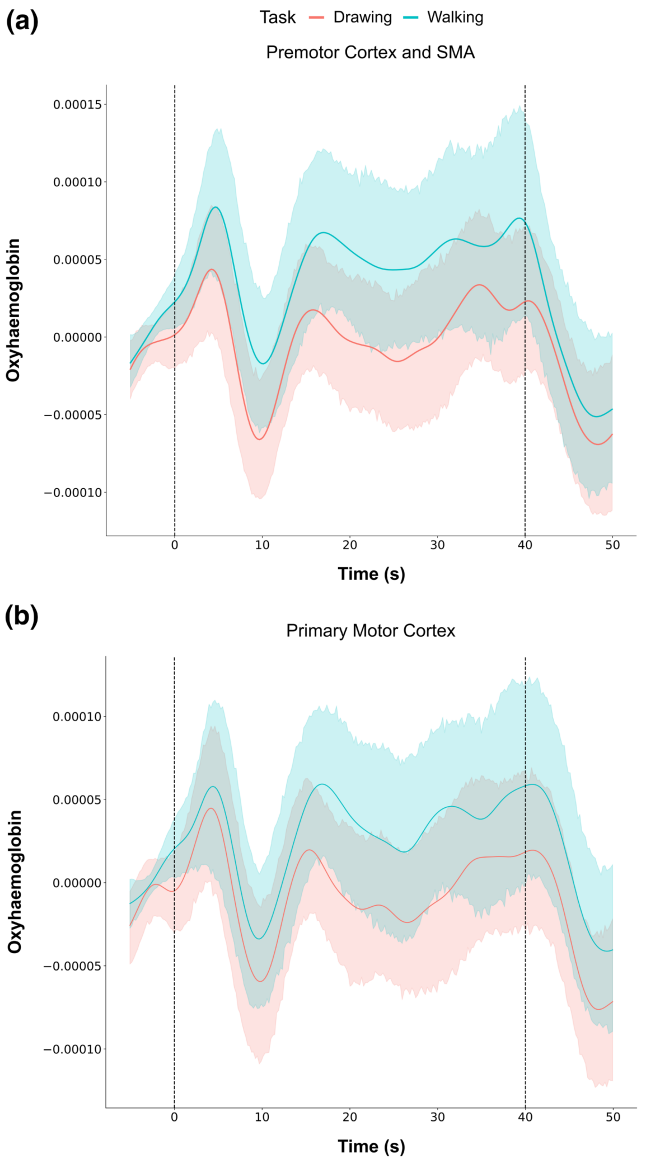

FIGURE 5 fNIRS results for the motor cortex. Mean oxyhemoglobin data for each designated task. 95% confidence intervals are represented by the shaded area that surrounds each trace. Panel A: Data for the premotor cortex and supplementary motor area (SMA). Panel: B Data for the primary motor cortex

in the close-to-spontaneous pace condition (r = .66, $t(13) = 3.13$, $p = .008$, $r^2 = .43$), but not in the slow ($r = .42$, $t(13) = 1.67$, $p = .118$, $r^2 = .18$) and fast pace conditions ($r = -.29$, $t(13) = -1.11$, $p = .288$, $r^2 = .09$). In addition, the correlation between the oxygenation levels of the the premotor cortex and SMA, and left dorsolateral prefrontal cortices was significant in the slow ($r = .76$, $t(13) = 4.21$, $p = .001$, $r^2 = .58$) and close-to-spontaneous pace condition ($r = .72$, $t(13) = 3.73$, $p = .002$, $r^2 = .52$), but not in the fast pace condition ($r = .45$, $t(13) = 1.83$, $p = .090$, $r^2 = .20$).

3.4.2 | Lateralization of prefrontal activations

To examine the lateralization of the prefrontal activity, additional two-way RM ANOVAs (Motor Tempo [300, 600, 1200 ms] × Task [drawing, walking]) were applied to $\overline{\Delta}_{HbO_2}$ for each brain hemisphere separately (i.e., left and right).

In the orbitofrontal cortex, the RM ANOVA was significant for both the left, $F(2, 22) = 7.88$, $p = .003$, $\eta_p^2 = .42$, and right hemispheres, $F(2, 22) = 3.53$, $p = .047$, $\eta_p^2 = .24$. Post hoc tests indicated that the orbitofrontal cortex oxygenation was greater in the 1200 vs. 300 ms ISI conditions only during the walking task ($p_{left} = .005$, $d_{left} = 1.08$, $p_{right} = .006$, $d_{right} = 1.08$).

In the dorsolateral prefrontal cortex, only the RM ANOVA conducted on the left hemisphere was significant, $F(2, 22) = 6.20$, $p = .007$, $\eta_p^2 = .36$. Post hoc tests indicated that the left-dorsolateral cortex oxygenation was greater in the 1200 vs. 300 ms ISI conditions only during the walking task ($p = .012$, $d = 1.00$; see Figure 7). The RM ANOVA conducted on the right hemisphere was nonsignificant, $F(2, 22) = 1.84$, $p = .183$, $\eta_p^2 = .143$.

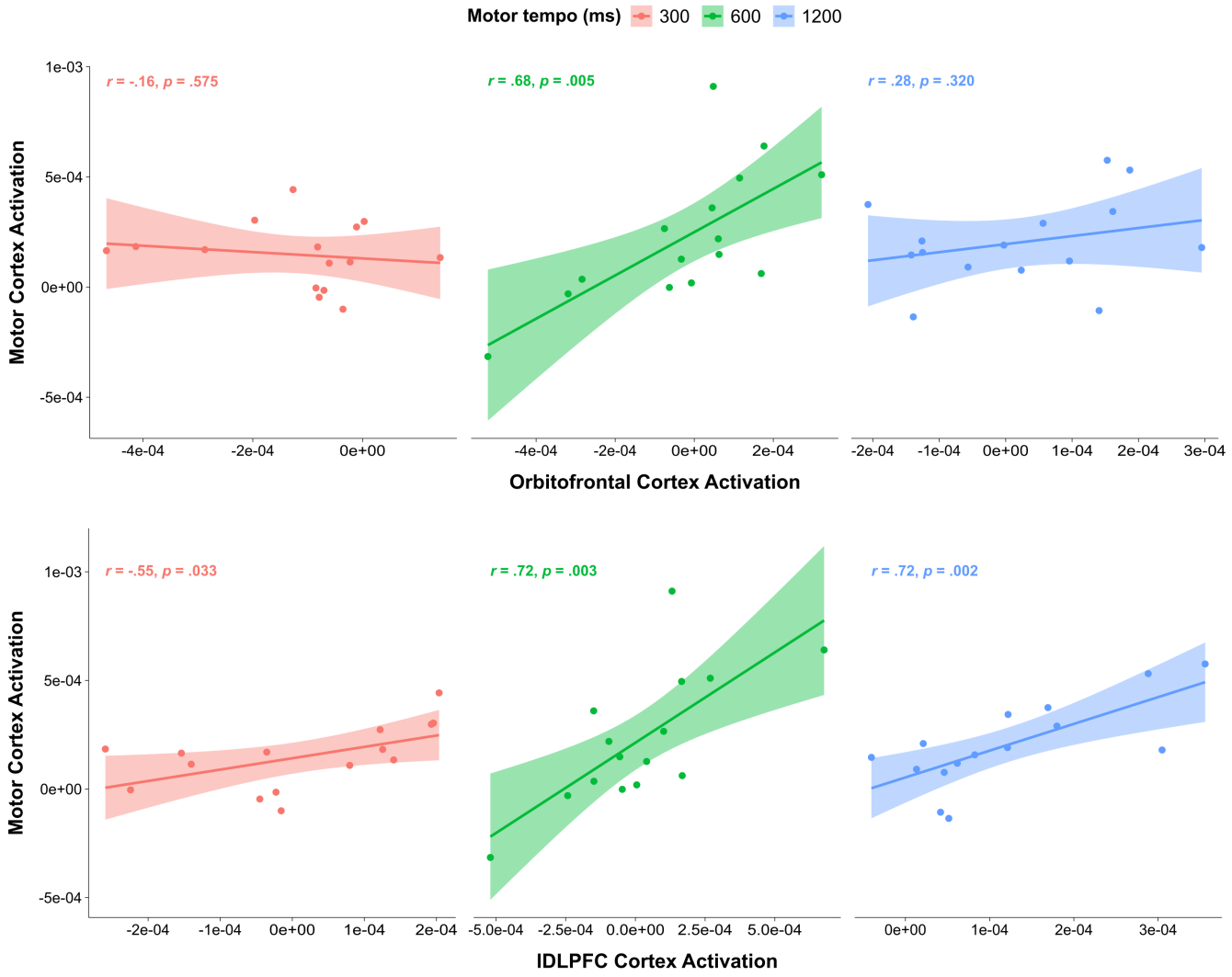

FIGURE 6 Correlation between prefrontal and motor oxygenation. Linear regression lines and associated 95% confidence intervals are displayed for each designated motor tempo. Panel A: Data for the obitofrontal cortex. Panel B: Data for the left dorsolateral prefrontal cortex (lDLPFC)

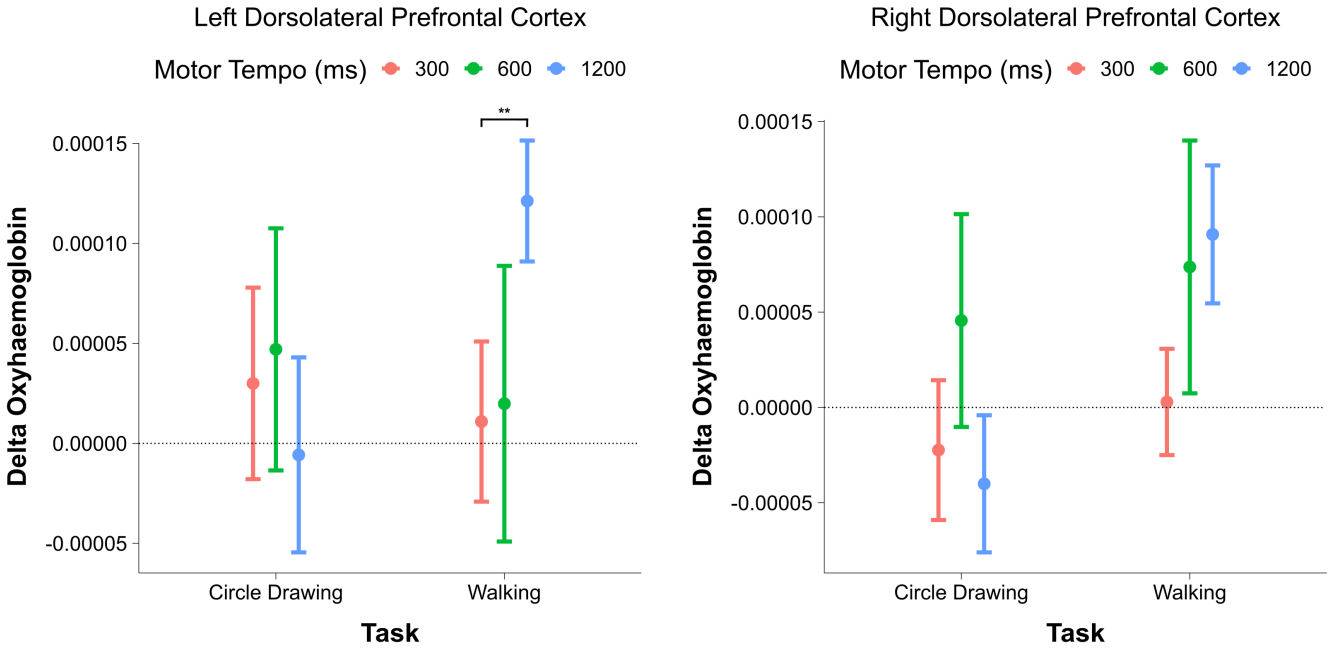

FIGURE 7 *f*NIRS results for the left and right dorsolateral prefrontal cortex. Mean oxyhemoglobin data for each designated tempo and task. 95% confidence intervals are represented by the error bars attached to each mean point. $^{**}p < .010$

3.4.3 | Beginning vs. end of trials

To examine the HbO_2 dynamics over the course of a trial, additional two-way RM ANOVAs (Motor Tempo [300, 600, 1200 ms] × Period [beginning, end]) were applied to $\overline{\Delta}_{HbO_2}$ for each task separately. The value for the end of a trial was computed as the mean $\overline{\Delta}_{HbO_2}$ value over the last 5 s, as previously computed. The value for the beginning of a trial was calculated as the mean $\overline{\Delta}_{HbO_2}$ over the first 10–15 s.[2] In the interest of conciseness, only the significant main effect and interaction of period are reported.

Prefrontal cortex

For the drawing task, the RM ANOVA showed a significant Motor Tempo × Period interaction in the bilateral orbitofrontal, $F(2, 22) = 4.89$, $p = .017$, $\eta_p^2 = .31$, and left dorsolateral prefrontal cortices, $F(2, 22) = 3.58$, $p = .045$, $\eta_p^2 = .27$. Nonetheless, the post hoc tests were nonsignificant. For the steady-state walking task, the RM ANOVA did not show any significant effects of period.

Motor cortex

For the drawing task, the RM ANOVA showed a significant Motor Tempo × Period interaction in the primary motor cortex, $F(2, 22) = 4.14$, $p = .030$, $\eta_p^2 = .27$, and premotor cortex and supplementary motor area, $F(2, 22) = 4.90$, $p = .017$, $\eta_p^2 = .31$. Nonetheless, the post hoc tests were nonsignificant for the two regions of interest.

For the steady-state walking task, the RM ANOVA showed a significant main effect of period in the primary motor cortex, $F(1, 14) = 8.43$, $p = .012$, $\eta_p^2 = .38$, and premotor cortex and supplementary motor areas, $F(1, 14) = 5.48$, $p = .035$, $\eta_p^2 = .28$. This indicated higher HbO_2 concentration for the end vs. beginning ($d_{premotor} = 0.48$, $d_{motor} = 0.56$) of trials across the motor areas.

4 | DISCUSSION

The main purpose of the present study was to investigate prefrontal and motor brain activity during the execution of voluntary continuous movements at various tempi. Two motor tasks (i.e., drawing and steady-state walking) were employed in a sensorimotor-synchronization paradigm performed at fast (i.e., 300 ms), close-to-spontaneous (i.e., 600 ms), and slow paces (i.e., 1200 ms). The walking task led to greater motor oxygenation than the circle-drawing task. Accordingly, H_1 was verified. Action production at slow pace yielded more prefrontal activation when compared with action production at close-to-spontaneous and faster paces but this pattern was observed during the walking task only. Thus, H_2 was only partially confirmed and H_3 was verified. Finally, the slow tempi trials did not lead to less motor activity when compared the close-to-spontaneous and fast tempi trials. Hence, H_4 was not confirmed.

[2]This time range was chosen because it coincides with the beginning of the canonical haemodynamic response.

4.1 | Type of motor behaviors

The first major result reported here was the fact that both types of motor tasks did not yield similar behavioral and cerebral outcomes. Artificial movements (i.e., drawing) led to higher timing errors and were more affected by motor tempo than ecological daily motor activities (i.e., walking), which replicate our previous results (Rose et al., 2021). These findings resonate with the notion that walking is a phylogenetically old motor activity (i.e., found in many organisms and present quite early in the evolutionary development of humans). Thus, the pattern of movements peculiar to walking is deep-rooted in the brain circuitry and its production is completely automatic (Schaal et al., 2004). Modulating the pace of such usual patterns of body movements is relatively easy, which is not the case for less ingrained actions.

The larger timing errors observed in the drawing task were not associated with increased prefrontal activity. Thus, it may be presumed that performing and modulating the pace of upper-limb movements did not require additional cognitive resources when compared to whole-body movements. An alternative hypothesis is that whole-body motor behaviors benefited from higher entrainment (i.e., temporal locking process in which a signal frequency entrains the frequency of a system; Thaut, 2013). The entrainment process has indeed been shown to optimize motor planning and execution, possibly through spontaneous adjustments of neural dynamics (Nozaradan et al., 2011; Thaut et al., 2015). This notion is corroborated in the present study by the findings that greater motor oxygenation was observed during the execution of the walking when compared with the drawing task.

An interesting observation is that the premotor and primary motor areas displayed a similar pattern of results. Previous research has shown that the premotor area plays a key role in motor timing, while the primary motor region acts more as a vassal. More specifically, Long and Fee (2008) found that slowing the rate of the premotor nucleus affected the song speed of songbird, which was not the case of the motor nucleus. Thus, an explanation to the similar pattern of brain activity we obtained across the motor regions is that activity in the primary motor cortex mimic that of the premotor area during the timing of movements.

4.2 | HbO_2 concentration dynamics

An original contribution of the present study concerns the investigation of the hemodynamic response dynamics by contrasting brain activity at the beginning vs. end of the stimulation period. The primary motor cortex oxygenation was found to increase from the beginning to the end of the walking trials. These results are consistent with the findings reported in sport sciences and confirm that gradual increases in oxyhemoglobin level are observed during the execution of a motor task (e.g., Fumoto et al., 2010). Such cerebral phenomenon can be attributed to the filling of nutritional requirements in the motor regions of the brain. Notably, the progressive increased in nutritional requirements would be induced by the sustained activity of the motor neurons supporting muscular activity. This would explain the absence of a gradual rise in motor activity during the time course of the circle-drawing trials, which did not require a lot of muscular effort.

In the present study, the length of the experimental trials (i.e., 40 s) enabled the researchers to contrast HbO_2 concentration at the beginning vs. end of the motor task execution. Nonetheless, most of the studies using motor paradigms employed shorter trials (~15 s; e.g., Batula et al., 2017; Caçola et al., 2018; Curzel et al., 2021) that do not permit the investigation of hemodynamic activity over time. It is noteworthy that a time-locked dip is visible in the *f*NIRS signal across all the regions of interest ~10 s after the beginning of a trial (see Figure 5). As *f*NIRS knowledge stands, the source of such fluctuation is still unclear. Researchers usually take the first 5–20 s of the signal to infer brain activation (see e.g., Delorme et al., 2019; Iso et al., 2016), which is exactly where the fluctuation occurred. Thus, future researchers need to carefully consider the trial length that is most suitable in addressing their research hypotheses. Lengthy trials (e.g., > 30 s) might be useful to increase chances of reaching a plateau in the hemodynamic response and examine subtle variations in the pattern of cerebral activation observed over the course of a cognitive process.

4.3 | Dorsolateral prefrontal cortex supports the production of synchronized movements

It is notable that the prefrontal cortex (i.e., orbitofrontal and dorsolateral regions) was activated to a greater extent during the production of slow vs. fast movement, specifically during the whole-body walking task. Supplementary analyses showed that only the left part of the dorsolateral cortex was activated during the slow walking trials. It is the case that the dorsolateral prefrontal cortex plays a critical role in inhibition, planning, and working memory (Curtis & D'Esposito, 2003; Oldrati et al., 2016; Tanji & Hoshi, 2001). Nevertheless, the right and left part of these areas have been reported to provide specific functional contributions. The right dorsolateral prefrontal cortex was shown to be related to sustained attention and

learning processes (Mannarelli et al., 2015; Tomasino & Fabbro, 2016). The right dorsolateral prefrontal cortex was also found to be involved in time production especially in tasks for which decisions regarding the timing of movements were to be made (Jenkins et al., 2000). Nonetheless, the findings of the present study provide first evidence suggesting that the right dorsolateral prefrontal cortex does not play a sensitive role in the pacing of movements.

Activity in the left part of the dorsolateral prefrontal cortex has been related to inhibition of response *planning* rather than response *execution* (Kadota et al., 2010). Therefore, the left dorsolateral prefrontal cortex could support movement planning instead of motor inhibition per se. Notably, the left dorsolateral cortex has been also reported to be involved in goal prioritization and decision making (Kaller et al., 2011; Turnbull et al., 2019). For example, Heekeren et al. (2006) proposed that the left part of the dorsolateral prefrontal cortex acts as a "comparator" by integrating information from the motor and sensory areas to make decisions and guide subsequent behaviors. This notion is corroborated by the positive moderately-high correlations found in the present study between activation in the left dorsolateral prefrontal cortex and the primary motor cortex, regardless of motor pace.

When producing a movement at a slow pace, the integration of multidimensional information has time to be implemented, which is not the case when moving at fast tempi (see Guérin, Boitout, & Delevoye-Turrell, 2021). This could provide a plausible explanation for the enhanced left dorsolateral prefrontal activity observed in the present study during the slow walking trials. Consequently, we propose that the dorsolateral prefrontal cortex may be involved in the production of timed behaviors, but not necessarily in decreasing the pace of spontaneous movements. Future research would need to compare the involvement of the dorsolateral prefrontal cortex in synchronization vs. self-paced movements.

It should be emphasized that the increase in left dorsolateral prefrontal cortex during slow trials was observed only in the walking task. Research has shown that left-lateralized prefrontal activity is involved in fixed expectations (Coull et al., 2011; Friedman & Robbins, 2022), as it is the case during the sensorimotor synchronization task used in the present study. In perceptual timing studies, more left-sided activity was also reported in implicit tasks (e.g., temporal expectation) when compared with explicit tasks (e.g., duration estimation; Coull & Nobre, 2008). Because walking is a highly automatized behavior in healthy adults, the timing of such pattern of movements is assumed to be more implicit than in less automatized behaviors (e.g., upper-limb movements; see Rose et al., 2021), which would lead to higher left-hemisphere activation. Additional motor timing studies comparing different classes of movements are now needed to corroborate this hypothesis.

4.4 | Motor inhibition is underpinned by orbitofrontal activation

In the present study, the orbitofrontal and dorsolateral prefrontal cortices showed a similar trend in terms of brain activity. Nonetheless, it is important to note that only the left part of the dorsolateral prefrontal cortex was involved in the modulation of motor timing (see Figure 7). In particular, the left dorsolateral prefrontal cortex was found to modulate the dopamine release, which is of particular importance for timing and to mediate impulsiveness (Pine et al., 2010), in the orbitofrontal cortex. Thus, the similarity in terms of brain activation between these two prefrontal anatomically distinctive brain regions could be due to their strong functional connections (Cohen et al., 2005, see). More specifically, the left dorsolateral prefrontal cortex would be in charge of the decision making of when to move in order to offer optimal synchronization with the external cue. Thus, the left dorsolateral prefrontal cortex would not only send information to the motor cortex to initiate movement, but also to the orbitofrontal cortex to inhibit the spontaneous pace of movement.

In a previous study using *f*MRI, the orbitofrontal cortex was found to be active when participants performed a cognitive task requiring inhibition (Horn et al., 2003; Rubia et al., 2001). In addition, patients with focal lesions to the medial orbitofrontal cortex were significantly impaired during the inhibition of irrelevant responses (Szatkowska et al., 2007). Thus, the greater orbitofrontal activation found in the present study during slow walking trials suggests that inhibition is needed to produce movements slower than the spontaneous pace. More specifically, inhibitory control would be a key process in restraining the urge to move at spontaneous pace. As scientific knowledge stands, the neurobiological origin of the spontaneous motor tempo is still unknown to the scientific community (Morillon et al., 2019). Nonetheless, it could be that prefrontal inhibitory signals are sent to the motor neurons in order to decelerate the speed of neural trajectories in the motor regions (see Buonomano & Karmarkar, 2002).

The fact that this prefrontal phenomenon was found only during the walking task suggests that inhibitory control is particularly salient for locomotion (Mirelman et al., 2012; Yogev-Seligmann et al., 2008). It has been suggested that the temporal structure for a given movement is not transferable to another movement (Buonomano & Karmarkar, 2002). It is arguable that the walking behavior is so natural and

habitually performed that its neural trajectories are characterized by stronger synaptic weights when compared with less stereotyped behaviors. Thus, a larger degree of inhibitory control would be needed to decelerate the speed of the neural trajectories coding for locomotion.

Results of the present study showed that performing a task at slow pace did not induce less activity in the motor areas of the brain when compared with performing the same task at fast pace. This pattern of results is in contradiction with our previous results (Guérin, Vincent, et al., 2021). Nonetheless, in this previous study, we did not find similar effects of motor tempo across the finger-tapping and the circle-drawing tasks over the motor areas using equivalence testing. We re-analyzed data from this previous study using a one-way ANOVA (motor tempo [300 ms, 500 ms, 1200 ms]) applied to the two tasks separately, and we found greater motor activity in the 300 vs. 1200 ms trials *only* during the finger-tapping task. Thus, it could be that the larger increases in oxyhemoglobin frequently found over the motor cortex when a movement is executed at a fast pace (see e.g., Kuboyama et al., 2004, 2005) are specific to discrete tasks (e.g., finger tapping) but not found in continuous tasks (e.g., circle drawing, walking).

Another plausible hypothesis is that the production of fast and slow movements is not underlined by two distinct processes, as suggested in the scientific literature (e.g., Lewis & Miall, 2003a; Wiener et al., 2010). Rather, a unique timing mechanism could support the production of fast and slow movements. In the scope of the population-clocks model (Buonomano & Karmarkar, 2002), motor timing could be embedded within the cerebral cortex, the most likely candidate being the motor regions. Thus, the pace of motor behaviors would *emerge* from the dynamics of a population of motor neurons (Buonomano & Laje, 2011). The natural pace of motor behaviors (i.e., 2 Hz) could originate in an increased brain connectivity between the prefrontal and motor areas (see Figure 6), which could explain the motor facilitation effect traditionally observed at this particular rate (e.g., Delevoye-Turrell et al., 2014). An additional cognitive process—the most likely candidate being motor inhibition—would be required for the production of body movements slower than the spontaneous, natural tempo. This notion is supported by our recent findings showing that a smooth increase in the attentional resources needed to perform a motor task is observed as the movement of the arm is slowed down (Guérin, Boitout, & Delevoye-Turrell, 2021).

4.5 | Limitations and future directions

A limitation pertaining to the experimental paradigm used is that participants had to synchronize their motor responses with an auditory stimulus (i.e., beep). Such sensorimotor synchronization might have entailed distinct motor-timing processes than those engaged during self-paced actions. The left dorsolateral activation reported in the present study could be attributed to a by-product of the synchronization process rather than to the effect of motor tempo per se. More research is needed to provide a fuller picture of the prefrontal pattern of activity involved in motor timing and dissociate the specific contributions of the dorsolateral prefrontal and orbitofrontal cortices.

While the the *f*NIRS data were filtered to eliminate global systemic physiology (i.e., heart and respiratory rates), the absence of short channels must also be acknowledged as a limit. A final limitation lies with the apparent variability of our *f*NIRS signals (see Figure 5). Even if three trials are commonly used in *f*NIRS studies employing a block-design procedure (Menant et al., 2020), more trials might have been beneficial to reduce the variability of individual mean hemodynamic responses.

5 | CONCLUSIONS

When examined collectively, findings of the present study showed that whole-body movements (i.e., walking) led to a higher HbO_2 concentration over the motor regions when compared with upper-limb activities (i.e., circle drawing). In addition, more bilateral orbitofrontal and left dorsolateral activation were observed during the slow walking trials. We advocate that motor inhibition could be a key process to restrain the urge to move at spontaneous pace when producing automatic, whole-body motor behaviors. Moreover, the present results serve to evidence that caution must be taken when generalizing the results from upper-limb, laboratory-based tasks to daily motor activities.

AUTHOR CONTRIBUTIONS

Ségolène M. R. Guérin: Conceptualization; data curation; formal analysis; investigation; methodology; software; visualization; writing – original draft. **Marion A. Vincent:** Conceptualization; data curation; formal analysis; methodology; software; writing – review and editing. **Yvonne N. Delevoye-Turrell:** Conceptualization; funding acquisition; methodology; project administration; supervision; writing – original draft; writing – review and editing.

ACKNOWLEDGMENTS

The authors thank Dr. Laurent Ott for his technical support, Victor P. M. Brossard for his valuable input regarding data visualization, and all the participants involved in the study.

CONFLICT OF INTEREST

The authors have no competing financial interests to declare.

DATA AVAILABILITY STATEMENT

The study data and materials are shared openly as part of the publication of the article (https://doi.org/10.5281/zenodo.5147920). The study received financial support from ANR-11-EQPX-0023 and from CNRS 80PRIME-2020-KinAImotion.

ORCID

Ségolène M. R. Guérin https://orcid.org/0000-0003-0990-9408
Marion A. Vincent https://orcid.org/0000-0002-1761-7491
Yvonne N. Delevoye-Turrell https://orcid.org/0000-0003-4034-3684

REFERENCES

Albares, M., Lio, G., Criaud, M., Anton, J.-L., Desmurget, M., & Boulinguez, P. (2014). The dorsal medial frontal cortex mediates automatic motor inhibition in uncertain contexts: Evidence from combined *f*MRI and EEG studies. *Human Brain Mapping*, *35*(11), 5517–5531. https://doi.org/10.1002/hbm.22567

Baker, W. B., Parthasarathy, A. B., Busch, D. R., Mesquita, R. C., Greenberg, J. H., & Yodh, A. (2014). Modified beer-Lambert law for blood flow. *Biomedical Optics Express*, *5*, 4053–4075. https://doi.org/10.1364/BOE.5.004053

Batula, A. M., Mark, J. A., Kim, Y. E., & Ayaz, H. (2017). Comparison of brain activation during motor imagery and motor movement using *f*NIRS. *Computational Intelligence and Neuroscience*, *2017*, e5491296. https://doi.org/10.1155/2017/5491296

Bobin-Bègue, A., & Provasi, J. (2008). Régulation rythmique avant 4 ans: Effet d'un tempo auditif sur le tempo moteur [Rhythmic regulation before 4 years: Effect of an auditory tempo on the motor tempo]. *L'Année Psychologique*, *108*, 631–658. https://frama.link/78H2hbzN

Bobin-Bègue, A., Provasi, J., Marks, A., & Pouthas, V. (2006). Influence of auditory tempo on the endogenous rhythm of non-nutritive sucking. *European Review of Applied Psychology*, *56*, 239–245. https://doi.org/10.1016/j.erap.2005.09.006

Buonomano, D. V., & Karmarkar, U. R. (2002). How do we tell time? *The Neuroscientist*, *8*(1), 42–51. https://doi.org/10.1177/1073858402000800109

Buonomano, D. V., & Laje, R. (2011). Population clocks: Motor timing with neural dynamics. In S. Dehaene & E. M. Brannon (Eds.), *Space, time and number in the brain* (pp. 71–85). Elsevier. https://doi.org/10.1016/B978-0-12-385948-8.00006-2739

Caçola, P., Getchell, N., Srinivasan, D., Alexandrakis, G., & Liu, H. (2018). Cortical activity in fine-motor tasks in children with developmental coordination disorder: A preliminary *f*NIRS study. *International Journal of Developmental Neuroscience*, *65*, 83–90. https://doi.org/10.1016/j.ijdevneu.2017.11.001

Cohen, M., Heller, A., & Ranganath, C. (2005). Functional connectivity with anterior cingulate and orbitofrontal cortices during decision-making. *Cognitive Brain Research*, *23*(1), 61–70. https://doi.org/10.1016/j.cogbrainres.2005.01.010

Coull, J., & Nobre, A. (2008). Dissociating explicit timing from temporal expectation with *f*MRI. *Current Opinion in Neurobiology*, *18*(2), 137–144. https://doi.org/10.1016/j.conb.2008.07.011

Coull, J. T., Cheng, R.-K., & Meck, W. H. (2011). Neuroanatomical and neurochemical substrates of timing. *Neuropsychopharmacology*, *36*(1), 3–25. https://doi.org/10.1038/npp.2010.113

Coyle, S. M., Ward, T. E., & Markham, C. M. (2007). Brain–computer interface using a simplified functional near-infrared spectroscopy system. *Journal of Neural Engineering*, *4*, 219–226. https://doi.org/10.1088/1741-2560/4/3/007

Curtis, C. E., & D'Esposito, M. (2003). Persistent activity in the prefrontal cortex during working memory. *Trends in Cognitive Sciences*, *7*(9), 415–423. https://doi.org/10.1016/S1364-6613(03)00197-9

Curzel, F., Brigadoi, S., & Cutini, S. (2021). *f*NIRS & e-drum: An ecological approach to monitor hemodynamic and behavioural effects of rhythmic auditory cueing training. *Brain and Cognition*, *151*, 105753. https://doi.org/10.1016/j.bandc.2021.105753

Delevoye-Turrell, Y., Dione, M., & Agneray, G. (2014). Spontaneous motor tempo is the easiest pace to act upon for both the emergent and the predictive timing modes. *Procedia-Social and Behavioral Sciences*, *126*, 121–122. https://doi.org/10.1016/j.sbspro.2014.02.338

Delignieres, D., & Torre, K. (2011). Event-based and emergent timing: Dichotomy or continuum? A reply to Repp and Steinman (2010). *Journal of Motor Behavior*, *43*(4), 311–318. https://doi.org/10.1080/00222895.2011.588274

Delorme, M., Vergotte, G., Perrey, S., Froger, J., & Laffont, I. (2019). Time course of sensorimotor cortex reorganization during upper extremity task accompanying motor recovery early after stroke: An *f*NIRS study. *Restorative Neurology and Neuroscience*, *37*(3), 207–218. https://doi.org/10.3233/RNN-180877

Derosière, G., Alexandre, F., Bourdillon, N., Mandrick, K., Ward, T. E., & Perrey, S. (2014). Similar scaling of contralateral and ipsilateral cortical responses during graded unimanual force generation. *NeuroImage*, *85*, 471–477. https://doi.org/10.1016/j.neuroimage.2013.02.006

Fraisse, P. (1982). Rhythm and tempo. In D. Deutsch (Ed.), *The psychology of music* (pp. 149–180). Academic Press.

Friedman, N. P., & Robbins, T. W. (2022). The role of prefrontal cortex in cognitive control and executive function. *Neuropsychopharmacology*, *47*, 72–89. https://doi.org/10.1038/s41386-021-01132-0

Frith, C., & Dolan, R. (1996). The role of the prefrontal cortex in higher cognitive functions. *Cognitive Brain Research*, *5*(1–2), 175–181. https://doi.org/10.1016/S0926-6410(96)00054-7

Fumoto, M., Oshima, T., Kamiya, K., Kikuchi, H., Seki, Y., Nakatani, Y., Yu, X., Sekiyama, T., Sato-Suzuki, I., & Arita, H. (2010). Ventral prefrontal cortex and serotonergic system activation during pedaling exercise induces negative mood improvement and increased alpha band in EEG. *Behavioural Brain Research*, *213*(1), 1–9. https://doi.org/10.1016/j.bbr.2010.04.017

Gervain, J., Mehler, J., Werker, J. F., Nelson, C. A., Csibra, G., Lloyd-Fox, S., Shukla, M., & Aslin, R. N. (2011). Near-infrared spectroscopy: A report from the McDonnell infant methodology consortium. *Developmental Cognitive Neuroscience*, *1*, 22–46. https://doi.org/10.1016/j.dcn.2010.07.004

Guérin, S. M. R., Boitout, J., & Delevoye-Turrell, Y. N. (2021). Attention guides the motor-timing strategies in finger-tapping tasks when moving fast and slow. *Frontiers in Psychology*, *11*, 574396. https://doi.org/10.3389/fpsyg.2020.574396

Guérin, S. M. R., Vincent, M. A., Karageorghis, C. I., & Delevoye-Turrell, Y. N. (2021). Effects of motor tempo on frontal brain activity: An *f*NIRS study. *NeuroImage*, *230*, 117597. https://doi.org/10.1016/j.neuroimage.2020.117597

Heekeren, H. R., Marrett, S., Ruff, D. A., Bandettini, P., & Ungerleider, L. G. (2006). Involvement of human left dorsolateral prefrontal cortex in perceptual decision making is independent of response modality. *Proceedings of the National Academy of Sciences*, *103*(26), 10023–10028. https://doi.org/10.1073/pnas.0603949103

Hernandez, S. M., & Pollonini, L. (2020). NIRSplot: A tool for quality assessment of *f*NIRS scans. *Optics and the Brain 2020*. Optica Publishing Group. Paper BM2C–5. https://doi.org/10.1364/BRAIN.2020.BM2C.5

Herold, F., Wiegel, P., Scholkmann, F., & Müller, N. G. (2018). Applications of functional near-infrared spectroscopy (*f*NIRS) neuroimaging in exercise–cognition science: A systematic, methodology-focused review. *Journal of Clinical Medicine*, *7*(12), 466. https://doi.org/10.3390/jcm7120466

Herold, F., Wiegel, P., Scholkmann, F., Thiers, A., Hamacher, D., & Schega, L. (2017). Functional near-infrared spectroscopy in movement science: A systematic review on cortical activity in postural and walking tasks. *Neurophotonics*, *4*(4), e041403. https://doi.org/10.1117/1.NPh.4.4.041403

Horn, N., Dolan, M., Elliott, R., Deakin, J. F., & Woodruff, P. (2003). Response inhibition and impulsivity: An *f*MRI study. *Neuropsychologia*, *41*(14), 1959–1966. https://doi.org/10.1016/S0028-3932(03)00077-0

Iso, N., Moriuchi, T., Sagari, A., Kitajima, E., Iso, F., Tanaka, K., Kikuchi, Y., Tabira, T., & Higashi, T. (2016). Monitoring local regional hemodynamic signal changes during motor execution and motor imagery using near-infrared spectroscopy. *Frontiers in Physiology*, *6*, 416. https://doi.org/10.3389/fphys.2015.00416

Jasper, H. H. (1958). Report of the committee on methods of clinical examination in electroencephalography. *Electroencephalography and Clinical Neurophysiology*, *10*, 370–375. https://doi.org/10.1016/0013-4694(58)90053-1

Jenkins, I. H., Jahanshahi, M., Jueptner, M., Passingham, R. E., & Brooks, D. J. (2000). Self-initiated versus externally triggered movements: II. The effect of movement predictability on regional cerebral blood flow. *Brain*, *123*(6), 1216–1228. https://doi.org/10.1093/brain/123.6.1216

Kadota, H., Sekiguchi, H., Takeuchi, S., Miyazaki, M., Kohno, Y., & Nakajima, Y. (2010). The role of the dorsolateral prefrontal cortex in the inhibition of stereotyped responses. *Experimental Brain Research*, *203*(3), 593–600. https://doi.org/10.1007/s00221-010-2269-4

Kaller, C. P., Rahm, B., Spreer, J., Weiller, C., & Unterrainer, J. M. (2011). Dissociable contributions of left and right dorsolateral prefrontal cortex in planning. *Cerebral Cortex*, *21*(2), 307–317. https://doi.org/10.1093/cercor/bhq096

Kamran, M. A., Jeong, M. Y., & Mannan, M. (2015). Optimal hemodynamic response model for functional near-infrared spectroscopy. *Frontiers in Behavioral Neuroscience*, *9*, 151. https://doi.org/10.3389/fnbeh.2015.00151

Keele, S. W., Pokorny, R. A., Corcos, D. M., & Ivry, R. (1985). Do perception and motor production share common timing mechanisms: A correlational analysis. *Acta Psychologica*, *60*, 173–191. https://doi.org/10.1016/0001-6918(85)90054-X

Koechlin, E., Ody, C., & Kouneiher, F. (2003). The architecture of cognitive control in the human prefrontal cortex. *Science*, *302*(5648), 1181–1185. https://doi.org/10.1126/science.1088545

Kuboyama, N., Nabetani, T., Shibuya, K., Machida, K., & Ogaki, T. (2005). Relationship between cerebral activity and movement frequency of maximal finger tapping. *Journal of Physiological Anthropology and Applied Human Science*, *24*, 201–208. https://doi.org/10.2114/jpa.24.201

Kuboyama, N., Nabetani, T., Shibuya, K.-i., Machida, K., & Ogaki, T. (2004). The effect of maximal finger tapping on cerebral activation. *Journal of Physiological Anthropology and Applied Human Science*, *23*, 105–110. https://doi.org/10.2114/jpa.23.105

Lakens, D., Scheel, A. M., & Isager, P. M. (2018). Equivalence testing for psychological research: A tutorial. *Advances in Methods and Practices in Psychological Science*, *1*, 259–269. https://doi.org/10.1177/2515245918770963

Leff, D. R., Orihuela-Espina, F., Elwell, C. E., Athanasiou, T., Delpy, D. T., Darzi, A. W., & Yang, G.-Z. (2011). Assessment of the cerebral cortex during motor task behaviours in adults: A systematic review of functional near infrared spectroscopy (*f*NIRS) studies. *NeuroImage*, *54*, 2922–2936. https://doi.org/10.1016/j.neuroimage.2010.10.058

Lemoine, L. (2007). *Implication des processus de timing évènementiels et émergents dans la gestion des aspects temporels du mouvement* [Doctoral dissertation]. Université Montpellier 1.

Levin, O., Fujiyama, H., Boisgontier, M. P., Swinnen, S. P., & Summers, J. J. (2014). Aging and motor inhibition: A converging perspective provided by brain stimulation and imaging approaches. *Neuroscience & Biobehavioral Reviews*, *43*, 100–117. https://doi.org/10.1016/j.neubiorev.2014.04.001

Lewis, P. A., & Miall, R. C. (2003a). Overview: An image of human neural timing. In W. Meck (Ed.), *Functional and neural mechanisms of interval timing* (pp. 515–532). CRC Press. https://doi.org/10.1201/9780203009574.ch21

Lewis, P. A., & Miall, R. C. (2003b). Distinct systems for automatic and cognitively controlled time measurement: Evidence from neuroimaging. *Current Opinion in Neurobiology*, *13*, 250–255. https://doi.org/10.1016/S0959-4388(03)00036-9

Long, M. A., & Fee, M. S. (2008). Using temperature to analyse temporal dynamics in the songbird motor pathway. *Nature*, *456*(7219), 189–194. https://doi.org/10.1038/nature07448

MacDougall, H. G., & Moore, S. T. (2005). Marching to the beat of the same drummer: The spontaneous tempo of human locomotion. *Journal of Applied Physiology*, *99*(3), 1164–1173. https://doi.org/10.1152/japplphysiol.00138.2005

Mandrick, K., Derosiere, G., Dray, G., Coulon, D., Micallef, J.-P., & Perrey, S. (2013). Prefrontal cortex activity during motor tasks with additional mental load requiring attentional demand: A near-infrared spectroscopy study. *Neuroscience Research*, *76*(3), 156–162. https://doi.org/10.1016/j.neures.2013.04.006

Mannarelli, D., Pauletti, C., Grippo, A., Amantini, A., Augugliaro, V., Currà, A., Missori, P., Locuratolo, N., De Lucia, M. C.,

Rinalduzzi, S., & Fattapposta, F. (2015). The role of the right dorsolateral prefrontal cortex in phasic alertness: Evidence from a contingent negative variation and repetitive transcranial magnetic stimulation study. *Neural Plasticity*, *2015*, 410785. https://doi.org/10.1155/2015/410785

Mates, J., Müller, U., Radil, T., & Pöppel, E. (1994). Temporal integration in sensorimotor synchronization. *Journal of Cognitive Neuroscience*, *6*, 332–340. https://doi.org/10.1162/jocn.1994.6.4.332

Menant, J. C., Maidan, I., Alcock, L., Al-Yahya, E., Cerasa, A., Clark, D. J., de Bruin, E., Fraser, S., Gramigna, V., Hamacher, D., Herold, F., Holtzer, R., Izzetoglu, M., Lim, S., Pantall, A., Pelicioni, P., Peters, S., Rosso, A. L., George, R. S., … Mirelman, A. (2020). A consensus guide to using functional near-infrared spectroscopy in posture and gait research. *Gait & Posture*, *22*, 254–265. https://doi.org/10.1016/j.gaitpost.2020.09.012

Mirelman, A., Herman, T., Brozgol, M., Dorfman, M., Sprecher, E., Schweiger, A., Giladi, N., & Hausdorff, J. M. (2012). Executive function and falls in older adults: New findings from a five-year prospective study link fall risk to cognition. *PLoS One*, *7*(6), 40297. https://doi.org/10.1371/journal.pone.0040297

Moelants, D. (2002). Preferred tempo reconsidered. In D. G. Nair, E. W. Large, F. Steinberg, J. A. S. Kelso, K. Stevens, D. Burnham, & J. Renwick (Eds.), *Proceedings of the 7th international conference on music perception and cognition* (pp. 1–4). Causal Productions. https://biblio.ugent.be/publication/159578

Morais, G. A. Z., Balardin, J. B., & Sato, J. R. (2018). *f*NIRS optodes' location decider (fOLD): A toolbox for probe arrangement guided by brain regions-of-interest. *Scientific Reports*, *8*, 3341. https://doi.org/10.1038/s41598-018-21716-z

Morillon, B., Arnal, L. H., Schroeder, C. E., & Keitel, A. (2019). Prominence of delta oscillatory rhythms in the motor cortex and their relevance for auditory and speech perception. *Neuroscience & Biobehavioral Reviews*, *107*, 136–142. https://doi.org/10.1016/j.neubiorev.2019.09.012

Nozaradan, S., Peretz, I., Missal, M., & Mouraux, A. (2011). Tagging the neuronal entrainment to beat and meter. *Journal of Neuroscience*, *31*(28), 10234–10240. https://doi.org/10.1523/JNEUROSCI.0411-11.2011

Oldrati, V., Patricelli, J., Colombo, B., & Antonietti, A. (2016). The role of dorsolateral prefrontal cortex in inhibition mechanism: A study on cognitive reflection test and similar tasks through neuromodulation. *Neuropsychologia*, *91*, 499–508. https://doi.org/10.1016/j.neuropsychologia.2016.09.010

Pasley, B. N., & Freeman, R. D. (2008). Neurovascular coupling. *Scholarpedia*, *3*, 5340. https://doi.org/10.4249/scholarpedia.5340

Perrey, S. (2014). Possibilities for examining the neural control of gait in humans with *f*NIRS. *Frontiers in Physiology*, *5*, 204. https://doi.org/10.3389/fphys.2014.00204

Pine, A., Shiner, T., Seymour, B., & Dolan, R. J. (2010). Dopamine, time, and impulsivity in humans. *Journal of Neuroscience*, *30*(26), 8888–8896. https://doi.org/10.1523/JNEUROSCI.6028-09.2010

Pinti, P., Scholkmann, F., Hamilton, A., Burgess, P., & Tachtsidis, I. (2019). Current status and issues regarding pre-processing of *f*NIRS neuroimaging data: An investigation of diverse signal filtering methods within a general linear model framework. *Frontiers in Human Neuroscience*, *12*, 505. https://doi.org/10.3389/fnhum.2018.00505

Pollonini, L., Bortfeld, H., & Oghalai, J. S. (2016). PHOEBE: A method for real time mapping of optodes-scalp coupling in functional near-infrared spectroscopy. *Biomedical Optics Express*, *7*(12), 5104–5119. https://doi.org/10.1364/BOE.7.005104

Rae, C. L., Hughes, L. E., Anderson, M. C., & Rowe, J. B. (2015). The prefrontal cortex achieves inhibitory control by facilitating subcortical motor pathway connectivity. *Journal of Neuroscience*, *35*(2), 786–794. https://doi.org/10.1523/JNEUROSCI.3093-13.2015

Rahimpour, A., Pollonini, L., Comstock, D., Balasubramaniam, R., & Bortfeld, H. (2020). Tracking differential activation of primary and supplementary motor cortex across timing tasks: An *f*NIRS validation study. *Journal of Neuroscience Methods*, *341*, e108790. https://doi.org/10.1016/j.jneumeth.2020.108790

Repp, B. H. (2005). Sensorimotor synchronization: A review of the tapping literature. *Psychonomic Bulletin & Review*, *12*, 969–992. https://doi.org/10.3758/BF03206433

Repp, B. H., & Steinman, S. R. (2010). Simultaneous event-based and emergent timing: Synchronization, continuation, and phase correction. *Journal of Motor Behavior*, *42*(2), 111–126. https://doi.org/10.1080/00222890903566418

Rose, D., Ott, L., Guérin, S. M. R., Annett, L. E., Lovatt, P., & Delevoye-Turrell, Y. N. (2021). A general procedure to measure the pacing of body movements timed to music and metronome in younger and older adults. *Scientific Reports*, *11*(1), A3264. https://doi.org/10.1038/s41598-021-82283-4

Rubia, K., Russell, T., Overmeyer, S., Brammer, M. J., Bullmore, E. T., Sharma, T., Simmons, A., Williams, S. C., Giampietro, V., Andrew, C. M., & Taylor, E. (2001). Mapping motor inhibition: Conjunctive brain activations across different versions of go/no-go and stop tasks. *NeuroImage*, *13*(2), 250–261. https://doi.org/10.1006/nimg.2000.0685

Saling, L. L., & Phillips, J. G. (2007). Automatic behavior: Efficient not mindless. *Brain Research Bulletin*, *73*(1–3), 1–20. https://doi.org/10.1016/j.brainresbull.2007.02.009

Schaal, S., Sternad, D., Osu, R., & Kawato, M. (2004). Rhythmic arm movement is not discrete. *Nature Neuroscience*, *7*(10), 1136–1143. https://doi.org/10.1038/nn1322

Schmidt, R. A., Lee, T. D., Winstein, C., Wulf, G., & Zelaznik, H. N. (1988). *Motor control and learning: A behavioral emphasis* (6th ed.). Human Kinetics.

Shadgan, B., Molavi, B., Reid, W. D., Dumont, G., & Macnab, A. J. (2010). Do radio frequencies of medical instruments common in the operating room interfere with near-infrared spectroscopy signals? In T. Vo-Dinh, W. S. Grundfest, & A. Mahadevan-Jansen (Eds.), *Advanced biomedical and clinical diagnostic systems VIII* (pp. 1–6). SPIE BiOS. https://doi.org/10.1117/12.842712

Simonsohn, U. (2015). Small telescopes: Detectability and the evaluation of replication results. *Psychological Science*, *26*, 559–569. https://doi.org/10.1177/0956797614567341

Sonkusare, S., Breakspear, M., & Guo, C. (2019). Naturalistic stimuli in neuroscience: Critically acclaimed. *Trends in Cognitive Sciences*, *23*(8), 699–714. https://doi.org/10.1016/j.tics.2019.05.004

Sumner, P., & Husain, M. (2007). At the edge of consciousness: Automatic motor activation and voluntary control. *The Neuroscientist*, *14*(5), 474–486. https://doi.org/10.1177/1073858408314435

Szatkowska, I., Szymańska, O., Bojarski, P., & Grabowska, A. (2007). Cognitive inhibition in patients with medial orbitofrontal

damage. *Experimental Brain Research*, *181*(1), 109–115. https://doi.org/10.1007/s00221-007-0906-3

Tanji, J., & Hoshi, E. (2001). Behavioral planning in the prefrontal cortex. *Current Opinion in Neurobiology*, *11*(2), 164–170. https://doi.org/10.1016/S0959-4388(00)00192-6

Thaut, M. H. (2013). Entrainment and the motor system. *Music Therapy Perspectives*, *31*(1), 31–34. https://doi.org/10.1093/mtp/31.1.31

Thaut, M. H., McIntosh, G. C., & Hoemberg, V. (2015). Neurobiological foundations of neurologic music therapy: Rhythmic entrainment and the motor system. *Frontiers in Psychology*, *5*, 1185. https://doi.org/10.3389/fpsyg.2014.01185

Tomasino, B., & Fabbro, F. (2016). Increases in the right dorsolateral prefrontal cortex and decreases the rostral prefrontal cortex activation after-8 weeks of focused attention based mindfulness meditation. *Brain and Cognition*, *102*, 46–54. https://doi.org/10.1016/j.bandc.2015.12.004

Turnbull, A., Wang, H., Murphy, C., Ho, N., Wang, X., Sormaz, M., Karapanagiotidis, T., Leech, R., Bernhardt, B., Margulies, D., Vatansever, D., Jefferies, E., & Smallwood, J. (2019). Left dorsolateral prefrontal cortex supports context-dependent prioritisation of off-task thought. *Nature Communications*, *10*(1), 3816. https://doi.org/10.1038/s41467-019-11764-y

Wiener, M., Turkeltaub, P. E., & Coslett, H. B. (2010). Implicit timing activates the left inferior parietal cortex. *Neuropsychologia*, *48*(13), 3967–3971. https://doi.org/10.1016/j.neuropsychologia.2010.09.014

Yogev-Seligmann, G., Hausdorff, J. M., & Giladi, N. (2008). The role of executive function and attention in gait. *Movement Disorders*, *23*(3), 329–342. https://doi.org/10.1002/mds.21720

Zhu, W. (2012). Sadly, the earth is still round ($p < .05$). *Journal of Sport and Health Science*, *1*, 9–11. https://doi.org/10.1016/j.jshs.2012.02.002

SUPPORTING INFORMATION

Additional supporting information can be found online in the Supporting Information section at the end of this article.

Supinfo S1

Supinfo S2

How to cite this article: Guérin, S. M. R., Vincent, M. A., & Delevoye-Turrell, Y. N. (2023). Effects of motor pacing on frontal-hemodynamic responses during continuous upper-limb and whole-body movements. *Psychophysiology*, *60*, e14226. https://doi.org/10.1111/psyp.14226